

UOT 542.957:547.7:547.854

THERMAL STABILITY AND THERMODYNAMICS OF PYROLYSIS OF MONO-, BI-, AND TRINUCLEAR CARBINOL DERIVATIVES OF FERROCENE

A.I. Rustamova¹, Z.G. Gurbanov², Z.M. Mammadova¹, S.N. Osmanova¹, A.Kh. Guluzade¹,
A.N. Mammadov^{1,3}, E.H. Ismailov¹

¹*Institute of Catalysis and Inorganic Chemistry named after M.Naghiyev,
H.Javid Ave., 113, AZ1143, Baku, Azerbaijan;*

²*SOCAR Downstream Management, Baku; Azerbaijan;*

³*Azerbaijan Technical University,
H. Javid Ave. 25, AZ-1073 Baku, Azerbaijan
aygun.rustamova1601@gmail.com*

Received 19.05.2023

Accepted 19.07.2023

Abstract: Mono-, bi- and trinuclear carbinol derivatives of ferrocene $C_5H_5FeC_5H_4-C(CH_3)_2OH$ (I), $[C_5H_5FeC_5H_4]_2C(CH_3)OH$ (II), $[C_5H_5FeC_5H_4]_3C-OH$ (III) were synthesized. The thermal stability and thermodynamics of the pyrolysis of these compounds have been studied. The composition and structure of the synthesized compounds were established by elemental analysis (AAS, C, H analysis), 1H NMR, IR, and UV/visible spectroscopy. In the IR spectra of these compounds there are absorption bands with $\nu(OH) = 2910-3040\text{ cm}^{-1}$ and $\nu(OH) = 3080-3190\text{ cm}^{-1}$, and in the 1H NMR spectra there are absorption bands with chemical shift values $\delta(OH) = 4.29-4.18\text{ ppm}$ for OH groups that differ in position and are due to the formation of intra- and intermolecular associates with the participation of OH groups. The electronic absorption spectra indicate the presence of characteristic absorption bands in compounds I-III at $\lambda_{max} = 270$ (I), 278 (II), and 285 nm (III). It is shown that when samples are heated from room temperature to 700 °C in an inert gas flow, the residual mass of compounds I-III is 2.05, 20.24, and 66.96% of the initial mass, respectively, and these compounds decompose to form nanosized iron particles, iron oxide and carbon. The values of the melting temperature and saturation magnetization of nanosized iron particles formed during the pyrolysis of ferrocene and its derivatives I-III are calculated.

Keywords: ferrocene carbinol derivatives, thermal stability, pyrolysis

DOI: 10.32737/2221-8688-2023-3-251-261

1. Introduction

Due to their low toxicity and high thermal stability, ferrocene and its derivatives have found wide application in various fields of science and technology - the electronics industry, medicine, biochemistry, organic synthesis, and catalysis. Ferrocene and its derivatives are used in the creation of heat-resistant coatings and light-sensitive materials, liquid crystals, heat-resistant polymers, fuel combustion regulators, in the production of multilayer carbon nanotubes. Ferrocene is a promising starting material for obtaining iron oxide nanostructures by thermal decomposition, ferromagnetic micro/nanoparticles, thin films of

iron oxide, carbon nanotubes with ferromagnetic fillers, etc. [1-6]. The widespread use of ferrocene and its derivatives requires, first of all, the study of the features of reactions with their participation, in particular, the thermodynamics of pyrolysis and combustion reactions. The most complete information on thermodynamic properties and thermodynamic functions is available only for ferrocene and some of its derivatives [7-11]. The heat capacity of isobutanoylferrocene, benzoylferrocene, and benzylferrocene was measured in the temperature range from 6 K to 372 K by low-temperature adiabatic calorimetry in [8, 9]. In

[10] the heat capacities, entropy, enthalpy and free energy of formation were determined for a number of ferrocene derivatives - ferrocenylmethanol $C_5H_5FeC_5H_4-CH_2OH$, benzoylferrocene $C_5H_5FeC_5H_4-COC_6H_5$, benzylferrocene $C_5H_5FeC_5H_4-COC_6H_5$, propionylferrocene $C_5H_5FeC_5H_4-COC_2H_5$, n-propylferrocene $C_5H_5FeC_5H_4-C_3H_7$, isobutylferrocene $C_5H_5FeC_5H_4-CH_2CH(CH_3)_2$. In [12], the thermodynamics of ferrocene pyrolysis with the formation of iron clusters catalyzing the formation of carbon nanotubes is

presented, and an expression is obtained for the size distribution function of clusters depending on the conditions of their formation.

This paper presents the results of studying the composition, structure, thermal stability of ferrocene and its mono-, bi- and trinuclear derivatives - $C_5H_5FeC_5H_4C(CH_3)_2OH$ (I) $C_5H_5FeC_5H_4]_2C(CH_3)OH$ (II), $C_5H_5FeC_5H_4]_3C-OH$ (III), calculation of the temperature dependences of the thermodynamic parameters of the pyrolysis reactions of these compounds.

2. Objects and methods of research

The objects of study were ferrocene and its derivatives I-III.

2.1. Synthesis of ferrocene derivatives

The synthesis of the above ferrocene derivatives was carried out according to [13].

2.1.1. Synthesis of mononuclear dimethyl carbinol derivatives of ferrocene $C_5H_5FeC_5H_4-C(CH_3)_2OH$ (I).

For the synthesis of compound (I), a mixture of 0.1 mol of metallic lithium and 5 ml of mercury was intensively stirred at 50°C. 0.01 mol of ferrocene dissolved in 25 ml of tetrahydrofuran was added in portions to the amalgam thus obtained, and continuously stirred for 30 minutes. The obtained ferrosenyllithium intermediate $C_5H_5FeC_5H_4Li$ is easily oxidized and hydrolyzed. Decantation of the mixture was carried out by adding 8 ml of acetone, followed by stirring in a magnetic stirrer for 2-3 hours. Next, 3% HCl was added to the solution. After that, the color of the solution changed from light blue to light yellow and then remained unchanged. The reaction solution was then evaporated with heating to separate the desired product isopropylferrocenylcarbinol from the reaction mixture. After repeated washing of the residue with hot n-hexane (3-5 ml), it was extracted with 3-20 ml of ethanol. The extracts were mixed and the alcohol was removed. The residue was a light yellow compound $C_5H_5FeC_5H_4-C(CH_3)_2OH$ (I) with a melting point of 69-70°C and a yield of 87%. According to the results of elemental analysis, compound I corresponds to the general formula $C_{13}H_{16}FeO$. Calculated, %: Fe-22.96, C-63.93, H-6.55, O - 6.55. Found, %: Fe-22.48, C-63.05, H-6.37, O -

6.43. 1H NMR ($CDCl_3$): $\delta C_5H_5(\alpha, \beta)$ - 4.09 ppm; $\delta C_5H_4(\alpha, \beta)$ - 3.95; 3.80 ppm $\delta(OH)$ - 4.19 ppm $\delta(CH_3)$ - 2.25 ppm. IR spectrum: (KBr) $\nu(OH)$ - 3050; 3098 cm^{-1} . $\nu(C_5H_4)-C$ - 1105 cm^{-1} .

2.1.2. Synthesis of diferrosenylmonomethyl carbinol $[C_5H_5FeC_5H_4]_2C(CH_3)OH$ (II).

To do this, a 5% solution of NaOH in interval 0-10°C and further stirred for 0.5 hour. Then, a 3% HCl aqueous solution was added to the reaction mixture and extracted with n-hexane 3 times. To purify the dark brown residue from primary substances, it was washed with n-pentane or a light fraction of gasoline in a ratio of 3:10 (in ml). As a result, 3.44 g of dark brown carbinol derivative $[C_5H_5FeC_5H_4]_2C(CH_3)OH$ (II) was obtained. The yield of the target product with melting temperature 119-120 °C was 83%. According to the results of elemental analysis, the compound corresponds to the chemical formula $C_{22}H_{22}Fe_2O$. Calculated, %: C - 63.76, H - 5.31; Fe - 27.05, O-3.86. Found, %: C - 63.51; H - 5.25; Fe - 26.95, O - 3.79. 1H NMR ($CDCl_3$): δC_5H_5 - 4.08 ppm $\delta C_5H_4(\alpha, \beta)$ -3.79; 3.91 ppm $\delta(OH)$ - 4.29 ppm $\delta(CH_3)$ - 2.17 ppm. IR spectrum (KBr): $\nu(OH)$ -2995, 3032 cm^{-1} , $\nu(C_5H_4-C)$ - 1107 cm^{-1} .

2.1.3. Synthesis of trisferrosenyl carbinol $[C_5H_5FeC_5H_4]_3C-OH$ (III).

To 0.01 mol 5.72 g of trisferrocenylmonochloromethane $[C_5H_5FeC_5H_4]_3CCl$ and 100 ml of n-heptane were added 25 ml of 1.14 g of KOH diluted in 0.2 mol of water and stirred continuously for 30 min. As a result, a dark yellow (III) compound was obtained. The yield of this compound was

79%, melting point 142-143°C, decomposition $T_{\text{dec.}} > 296^\circ\text{C}$. According to the results of elemental analysis, the resulting compound corresponds to the chemical formula $\text{C}_{31}\text{H}_{28}\text{Fe}_3\text{O}$. Calculated, %: Fe-28.76, C - 63.69, H - 4.79, O - 2.73. Found, %: Fe-28.70, C - 63.50, H - 4.68, O - 2.63, ^1H NMR (CDCl_3): $\delta\text{C}_5\text{H}_5$ - 4.07 ppm, $\delta\text{C}_5\text{H}_4(\alpha, \beta)$ - 3.88; 3.96 ppm, $\delta(\text{OH})$ - 4.18 ppm. IR spectrum (KBr): $\nu(\text{OH})$ - 2965, 3022 cm^{-1} , $\nu(\text{C}_5\text{H}_4\text{-C})$ - 1107 cm^{-1} .

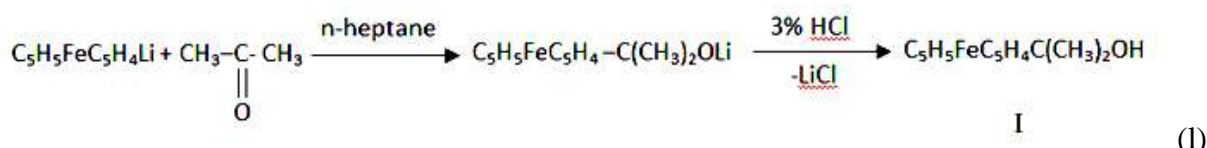
2.2. Methods for studying synthesized compounds

The elemental composition of the synthesized compounds was determined using an AAS iCE 3000 Thermo Fisher Scientific atomic absorption spectrometer and a LECO CHNOS analyzer, TruSpec Micro, USA. The structure of the synthesized compounds was established by IR and NMR spectroscopy. IR spectra were recorded on an Alfa Bruker IR Fourier spectrophotometer in KBr tablets; electronic absorption spectra of solutions of

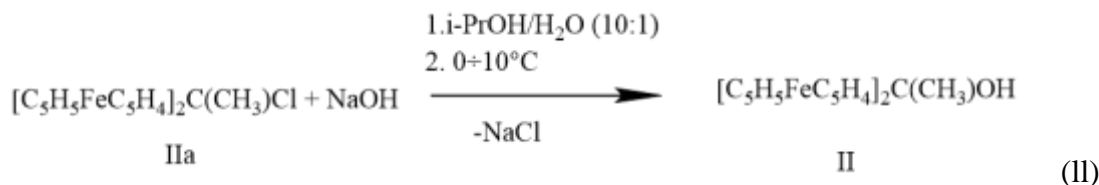
these compounds in organic solvents (n-hexane, heptane, acetone, ethyl alcohol) were recorded on a Specord 50 plus spectrophotometer, Jena Analytical, Germany. NMR spectra were recorded in deuterated acetone and chloroform at room temperature using an AM-300 spectrometer, Bruker with an operating frequency of 300 MHz. X-ray diffraction patterns were recorded using an XRD D2 PHASER diffractometer at room temperature. Thermal analysis experiments (TG/DTA) were carried out using a NETZSCH, F3 Jupiter, Germany thermal analyzer in dynamic mode in a nitrogen flow. A programmable temperature regime was used with a heating rate of 10°C per minute. In all TG/DTA experiments, about 10 mg of powders of ferrocene and its derivatives of the above composition were taken in a corundum crucible and subjected to thermal analysis in the temperature range from 20 to 700°C . Thermodynamic parameters were calculated using the Origin 2019 program.

3. Results and discussion

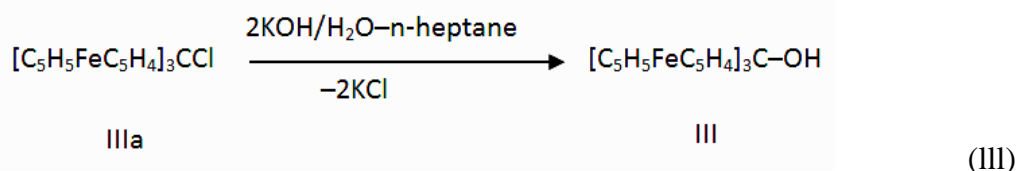
The mononuclear derivative of ferrocene, ferrocenyl-dimethylcarbinol $\text{C}_5\text{H}_5\text{FeC}_5\text{H}_4\text{C}(\text{CH}_3)_2\text{OH}$, was synthesized according to the following scheme [10]:



The binuclear derivative of ferrocene, bis-ferrocenylmonomethylcarbinol $[\text{C}_5\text{H}_5\text{FeC}_5\text{H}_4]_2\text{C}(\text{CH}_3)\text{OH}$ (II), was obtained with 83% yield by treating diferrocenylchloromethylmethane (IIa) with 5% NaOH in an aqueous isopropyl alcohol medium:



Using the chlorine derivative $[\text{C}_5\text{H}_5\text{FeC}_5\text{H}_4]_3\text{CCl}$ (IIIa) in the presence of KOH at a temperature of $0-10^\circ\text{C}$, compound III $[\text{C}_5\text{H}_5\text{FeC}_5\text{H}_4]_3\text{C-OH}$ was obtained with 79% yield.



The IR spectra of carbinols indicate the dependence of the intensity of OH groups on the structure of the carbinol. The bands with $\nu(\text{OH})$ 2668-2725 cm^{-1} are attributed to the OH group with an intramolecular bond with Fe. The bands located in the $\nu(\text{OH})$ range of 2910-3040 cm^{-1} are characteristic of associations of OH groups.

In the electronic absorption spectra, all three carbinols have shoulder-type absorption bands at: $\lambda_{\text{max}}=270$ nm: (I), $\lambda_{\text{max}}=278$ nm (II) and $\lambda_{\text{max}} 285$ nm (III).

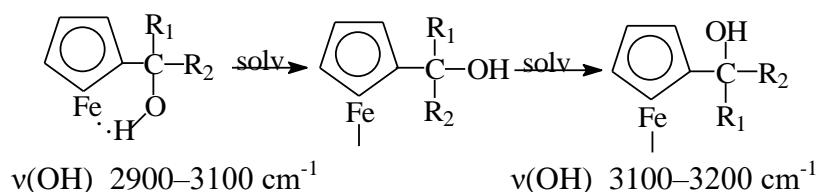
In table. 1 the ^1H NMR data for ferrocene and its derivatives were shown.

Table 1. Values of chemical shifts in the ^1H NMR spectra of ferrocene and ferrocenyl -carbinol compounds.

Compound	Chem.shift in C_5H_5 -ring, ppm.	Chem.shift in substituted C_5H_4 -, ppm			OH, ppm
		$\text{H}_{\alpha,\beta}$	CH_2	CH_3	
$(\text{C}_5\text{H}_5)_2\text{Fe}$	4.12				
$\text{C}_5\text{H}_5\text{FeC}_5\text{H}_4\text{-C}(\text{CH}_3)_2\text{OH}$	4.09	3.95; 3.80		2,25	4.19 tripl.
$\text{C}_5\text{H}_5\text{FeC}_5\text{H}_4\text{-CH}_2\text{-OH}$	3.95	3.80; 3.85	2.75		4.03 tripl.
$[\text{C}_5\text{H}_5\text{FeC}_5\text{H}_4]_2\text{C}(\text{CH}_3)\text{OH}$	4.08	3.79; 3.91		2,17	4.11 dubl.
$[\text{C}_5\text{H}_5\text{FeC}_5\text{H}_4]_3\text{COH}$	4.07	3.88; 3.96			4.18 tripl.

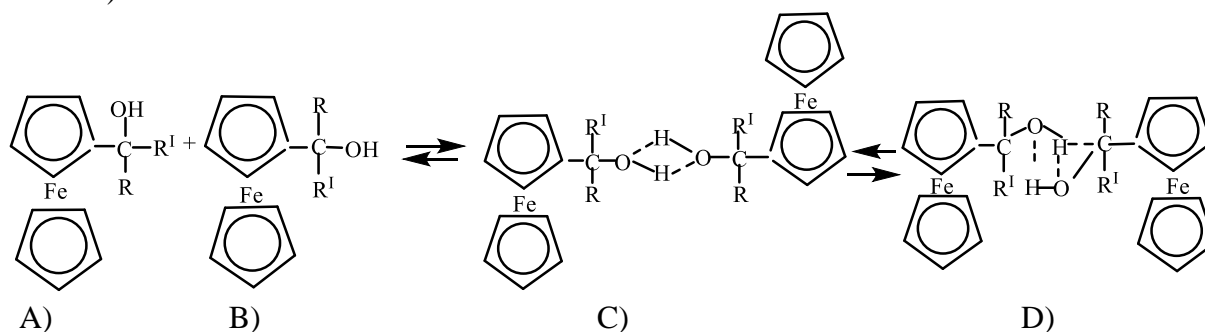
^1H NMR spectra indicate the presence of OH groups differing in position in these compounds. As can be seen from the table, the presence of different protons (H_α and H_β) in the cyclopentadiene radicals is due to the introduction of an OH group into the

ferrocenylcarbinol complexes. For the OH group in these compounds, two extreme positions can be realized. The bond of the central Fe atom with the hydrogen of the OH group can be broken by the action of solvating solvents (Scheme 1).



Scheme 1. Intramolecular coordination bond of the OH group proton with the Fe atom in carbinol derivatives of ferrocene and its elimination by the action of solvating solvents.

Below is a diagram of inter- and intramolecular rearrangements in ferrocenylcarbinols (Scheme 2).

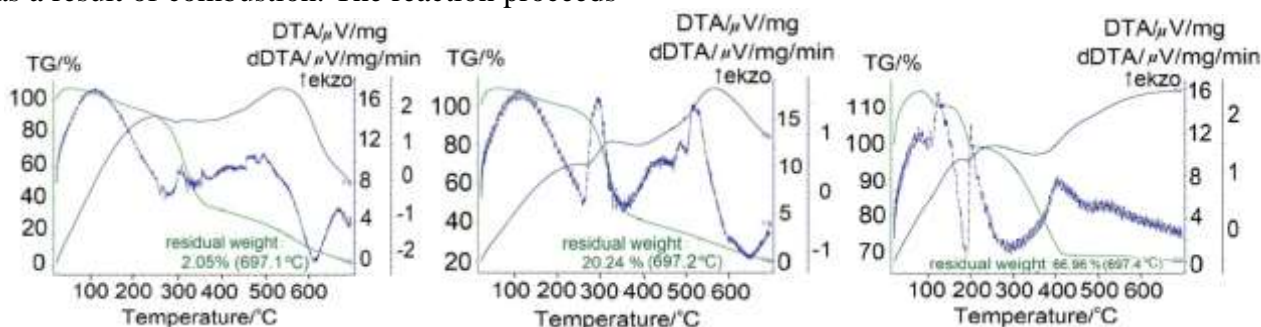


Scheme 2. Inter- and intramolecular rearrangements in ferrocenylcarbinols

As can be seen from the scheme, intermolecular interaction between (A) and (B) is resulted with the formation of the structure (C), which is in dynamic equilibrium with the D structure: $C \leftrightarrow D$. This equilibrium is realized between the structures of the intramolecular grouping.

Ferrocene is stable in air and does not decompose when heated to 743 K. Starting from 770 K, ferrocene decomposes intensively in air as a result of combustion. The reaction proceeds

with the formation of iron(III) oxide and the release of carbon dioxide and water into the gas phase. The synthesized derivatives of ferrocenylcarbinol I-III melt and decompose at lower temperatures than ferrocene. The final pyrolysis products of ferrocenylcarbinols are mainly the carbonized formation of cyclopentadienyl and iron(II) oxide. Figure 1, a-c shows thermograms of ferrocenylcarbinol compounds I-III.



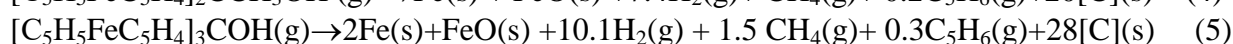
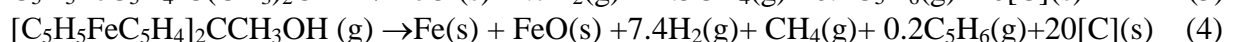
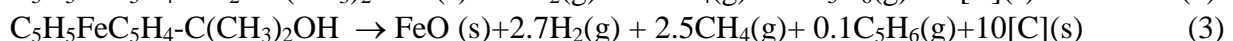
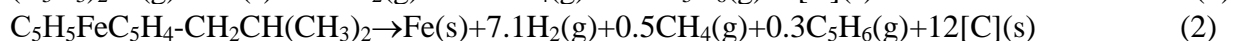
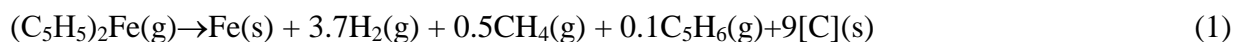
a) $C_5H_5FeC_5H_4C(CH_3)_2OH$ b) $[C_5H_5FeC_5H_4]_2C(CH_3)OH$ c) $[C_5H_5FeC_5H_4]_3C-OH$

Fig. 1. Thermograms of ferrocenylcarbinol compounds: a) I, b) II and c) III.

Thermograms of fig.1, a-c show that, unlike ferrocene, the above-mentioned derivatives decompose not in one stage, but at least in three stages. And the temperature intervals of thermal decomposition of compounds I-III are determined by the features of their composition and structure. The formation of iron(II) oxide as the final product during the thermal decomposition of ferrocene derivatives with oxygen-containing ligands is due to the oxidation of iron by these ligands formed during their thermal decomposition.

Above 770 K in an inert medium, ferrocene and its derivatives with hydrocarbon ligands decompose, forming particles of iron and carbon. The resulting carbon formation is almost 50% by weight and most likely represents a multiwalled nanocarbon tube [9, 10]. As can be seen from the thermograms shown in Fig. 1, when the samples are heated

from room temperature to 700 °C in an inert gas flow, the residual mass for compounds I-III is, respectively, 2.05, 20.24, and 66.96% of the initial mass. And if we assume that the residue of thermal decomposition of compounds I-III consists of a mixture of iron, iron oxides and carbon, then, in accordance with equations (3) - (5), the mass of the solid residue should be, respectively, 78.69, 88.89 and 89.04% of the initial mass. This circumstance is mainly due to the difference in the volatility of compounds I-III. Under the conditions of the experiment, when heated from room temperature to 700 °C in an inert gas flow, at least 76, 68 and 22% of the initial mass of compounds I-III flies, respectively. The pyrolysis of ferrocene and its derivatives under the above conditions can most likely be represented in the form of the following equations:



To determine the temperature dependences of the free energy of these reactions, the Ulich equation was used, which, despite its simple form, has a fairly high reliability [14, 15]:

$$\Delta G_T^0 = \Delta H_T^0 - T\Delta S_{298}^0 - \Delta C_{P,298}^0 T \left[\ln \left(\frac{T}{298} \right) + \frac{298}{T} - 1 \right] \quad (6)$$

In equations (6): ΔG_T^0 ; ΔH_T^0 ; ΔS_{298}^0 - free energies, enthalpies and entropies of reactions; which are determined on the basis of the thermodynamic functions of the substances involved in the reactions. $\Delta C_{p,298}^0$ is the difference between the molar isobaric heat capacities of the products and initial substances of the reactions. The thermodynamic parameters of ferrocene and derivatives are borrowed from [9, 10]; (Table 2).

Table 2. Thermodynamic parameters of ferrocene and its derivatives [8, 9].

Compound	$\Delta S_{298}^0(g)$, J/(K mol)	$\Delta H_{298}^0(g)$, kJ/mol	$\Delta G_{298}^0(g)$, kJ/mol	$C_{P,298}^0(g)$, J/(K mol)
Ferrocene (C ₅ H ₅) ₂ Fe	-3718 ± 26	230 ± 6	3387 ± 10	*255.9 ± 6
Ferrocenylmethanol C ₅ H ₅ FeC ₅ H ₄ -CH ₂ OH	-5147 ± 26	52 ± 10	205 ± 10	199 ± 5
Isobutylferrocene C ₅ H ₅ FeC ₅ H ₄ -CH ₂ CH(CH ₃) ₂	-7654 ± 20	133 ± 10	361 ± 10	255 ± 5
Monoferrocenyl dimethyl carbynol C ₅ H ₅ FeC ₅ H ₄ -C(CH ₃) ₂ OH	-6396 ± 26	98 ± 10	267 ± 10	232 ± 5
Diferrocenylmonomethyl carbynol (**) [C ₅ H ₅ FeC ₅ H ₄] ₂ C(CH ₃)OH	-1037 ± 30	655 ± 20	964 ± 25	578 ± 10
Triferrocenylcarbinol (**) [C ₅ H ₅ FeC ₅ H ₄] ₃ COH	-1445 ± 30	982 ± 20	1446 ± 30	763 ± 10

*This value is estimated according to the Neumann-Kop rule [16,17]; **Thermodynamic parameters of the noted compounds were estimated based on the thermodynamic parameters of ferrocene and ligands, taking into account their conversion to the corresponding radicals.

The thermodynamic parameters of other substances involved in reactions (1-5) are borrowed from [15]. Thermodynamic parameters for carbon nanotubes are taken from [7]. The following quantities were used in the calculations:

$$\begin{aligned} \Delta H_{298}^0 [(C_5H_5)_2Fe (g)] &= 230 \pm 6 \text{ kJ/mol}; \quad \Delta H_{298}^0 [(C_5H_6) (g)] = 105.9 \pm 1 \text{ kJ/mol} \\ \Delta H_{298}^0 [(CH_4(g))] &= -74.85 \text{ kJ/mol}; \quad \Delta H_{298}^0 [C(s)] = -2.03 \text{ kJ/mol} \\ \Delta H_{1000}^0 [C(s)] &= -1.98 \text{ kJ/mol}; \quad \Delta H_{298}^0 [(H_2(g))] = 0; \quad \Delta H_{298}^0 [\alpha-Fe] = 0 \\ \Delta S_{298}^0 [(C_5H_5)_2Fe (g)] &= -371.8 \pm 2.6 \text{ J/(mol.K)}; \quad S_{298}^0 [(C_5H_5)_2Fe (g)] = 361.1 \pm 2.1 \text{ J/(mol.K)} \\ \Delta S_{298}^0 [(C_5H_6) (g)] &= -237.8 \text{ J/(mol.K)}; \quad S_{298}^0 [(C_5H_6) (g)] = 182.7 \text{ J/(mol.K)} \\ \Delta S_{298}^0 [(CH_4(g))] &= -80.0 \text{ J/(mol.K)}; \quad S_{298}^0 [(CH_4(g))] = 186.19 \pm 85 \text{ J/(mol.K)} \\ \Delta S_{298}^0 [C(s)] &= 0.44 \text{ J/(mol.K)}; \quad \Delta S_{1000}^0 [C(s)] = 0.55 \text{ J/(mol.K)}; \quad S_{298}^0 [C(s)] = 6.25 \text{ J/(mol.K)} \\ \Delta S_{298}^0 [(H_2(g))] &= 0; \quad S_{298}^0 [(H_2(g))] = 130.6; \quad \Delta S_{298}^0 [\alpha-Fe] = 0; \quad S_{298}^0 [\alpha-Fe] = 27.5 \text{ J/(mol.K)} \\ C_{P,298}^0 [(C_5H_5)_2Fe (g)] &= 255.9 \text{ J/(mol.K)} - \text{calculation} \end{aligned}$$

The equations for the temperature dependence of the Gibbs energy of the pyrolysis reaction of ferrocene and its derivatives (reactions 1-5) are given in Table 3, Fig.2 and visualized in Fig. 3.

Table 3. Equations for the temperature dependence of the Gibbs energy of the reaction of pyrolysis of ferrocene and its derivatives (reactions 1-5), obtained by equation (6). The equations are presented in computerized form.

Reaction	Compound	Equation $\Delta G_T^0(\text{kJ/mol})=f(x)$; $x=T$
1	$(\text{C}_5\text{H}_5)_2\text{Fe}$	$-274.655-0.313 *x-0.0982*x*(\ln(x/298)+298/x-1)$
2	$\text{C}_5\text{H}_5\text{FeC}_5\text{H}_4-\text{CH}_2\text{CH}(\text{CH}_3)_2$	$-162-0,660*x-0,255*x*(\ln(x/298)+298/x-1)$
3	$\text{C}_5\text{H}_5\text{FeC}_5\text{H}_4-\text{C}(\text{CH}_3)_2\text{OH}$	$-364.8-0,2582*x-0,0756*x*(\ln(x/298)+298/x-1)$
4	$[\text{C}_5\text{H}_5\text{FeC}_5\text{H}_4]_2\text{C}(\text{CH}_3)\text{OH}$	$-1014+0,425*x+0,0549*x*(\ln(x/298)+298/x-1)$
5	$[\text{C}_5\text{H}_5\text{FeC}_5\text{H}_4]_3\text{COH}$	$-1383+0,242*x+0,036*x*(\ln(x/298)+298/x-1)$

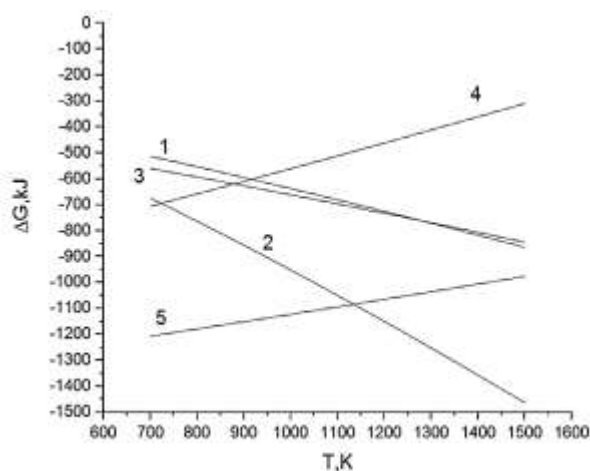


Fig. 2.

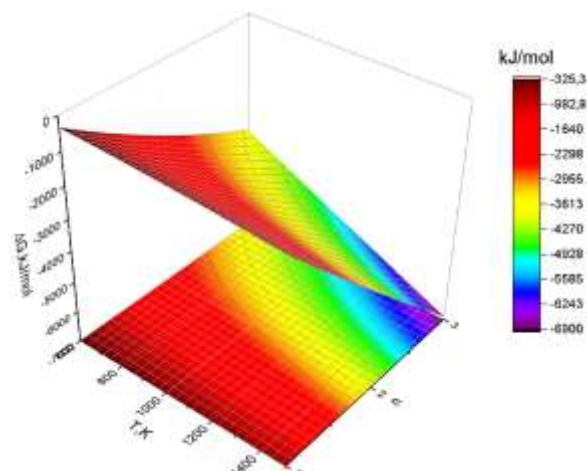


Fig.3.

Fig. 2. Temperature dependences of the Gibbs energy of pyrolysis reactions (1-5) of ferrocene and its derivatives.

Fig.3. 3D visualization of the dependence of the free energy of the pyrolysis reactions of ferrocene and its derivatives (1-5) on temperature and the number of ferrocene cores based on the equations given in table 3 and equation (7).

$$\Delta G_{298}^0(\text{kJ/mol}) = 588.5-1068.75*y + 139.75*y^2 + (2.639-2,6965*y + 0.1695*y^2)*x + (-1,639+1.475*y-0.277*y^2)*x*(\ln(x/298)+298/x-1) \quad (7)$$

From Fig. 2 it follows that the pyrolysis reactions of ferrocene and its derivatives (1-5) with the production of carbon structures in the range of 700-1500K are characterized by negative values of free energy. The reactions are endothermic. Reactions (1,2) with the production of iron (1) and iron oxide (2) proceed with an increase in entropy. Consequently, with increasing temperature, their negative values of free energy increase. Reactions with the simultaneous production of iron and iron oxide proceed with a decrease in entropy, therefore, with increasing temperature,

the negative values of their free energy greatly decrease.

Figure 3 visualizes the dependence of the free energy of pyrolysis on temperature in the range of 700-1600 K and on the number of ferrocene cores, respectively, for one-, two- and three-nuclear ferrocene compounds $\text{C}_5\text{H}_5\text{FeC}_5\text{H}_4-\text{CH}_2\text{OH}$, $[\text{C}_5\text{H}_5\text{FeC}_5\text{H}_4]_2\text{CCH}_3\text{OH}$, $[\text{C}_5\text{H}_5\text{FeC}_5\text{H}_4]_3\text{COH}$. Depending on the number of nuclei, the negative values of the pyrolysis free energy increase from -300 kJ/mol to -3000 kJ/mol.

As noted above, the pyrolysis of ferrocene results in the formation of iron nanoclusters with a diameter of less than 10 nm [12]. Below are the results of estimating the

melting temperature and saturation magnetization for spherical particles 10 nm in diameter using the melting temperature dependence equations [18], respectively,

$$T^m(r) = T^m [(1 - 2\sigma_{s-l})/(\Delta H^m \rho_s r)] \quad (8),$$

where T^m and $T^m(r)$ are the melting points, respectively, of a bulk sample and a nanoparticle with radius r ; $\sigma_{(s-l)}$ - surface tension

at the solid-liquid interface, ΔH^m - melting enthalpy, and saturation magnetization [19],

$$M_s = M_{sb}(1 - 2\delta/D)^3 \quad (9)$$

where M_{sb} is the saturation magnetization of the bulk material, D is the diameter of the magnetic particle, δ is the thickness of the skin layer.

For bulk iron $T_m = 1812$ K (1539 °C), $\sigma_{(s-l)} = 1.85 \cdot 10^{-4}$ J/cm², $\Delta H^m = 13.8$ kJ/mol = 246 J/g, $\rho_s = 7.87$ g/cm³. For a nanoparticle with a diameter of 10 nm, according to equation (8), we obtain the value of the melting point equal to 1228 K (953 °C). This is much less than the melting point of massive iron, 1812 K (1539 °C). For iron particles with a diameter of 20, 10 and 5 nm, the saturation magnetization will change

as follows: $1.627 \cdot 10^6$ A/m (20 nm), $1.513 \cdot 10^6$ A/m (10 nm), $1.301 \cdot 10^6$ A/m (5 nm), respectively, in the case of the assumption of a spherical shape of iron particles and the following values $M_{sb} = 1.747 \cdot 10^6$ A/m, and $\delta = 0.234 \cdot 10^{-9}$ m. As can be seen from the above calculations, the values of both the melting temperature and the saturation magnetization change with the change in the size of the iron particles. It should be noted that with a change in the size of iron particles, its catalytic activity in the reaction of formation of carbon structures will change.

Conclusion

One-, two- and three-nuclear carbinol derivatives of ferrocene $C_5H_5FeC_5H_4-C(CH_3)_2OH$ (I), $[C_5H_5FeC_5H_4]_2C(CH_3)OH$ (II), $[C_5H_5FeC_5H_4]_3C-OH$ (III) have been synthesized. It has been established that these compounds have lower melting points than ferrocene and are readily soluble in many organic solvents. It is shown that when the samples are heated from room temperature to 700 °C in an inert gas flow, the residual mass of compounds I-III is 2.05, 20.24 and 66.96% of

the initial mass, respectively, and these compounds decompose with the formation of nanosized iron particles, iron oxide and carbon. The values of the melting temperature and saturation magnetization of nanosized iron particles formed during the pyrolysis of ferrocene and its derivatives I-III are calculated. These compounds are supposed to be used as precursors for the production of iron-containing catalysts on carbon and oxide supports with nanosized active components.

References

1. Werner H (June 2012). "At least 60 years of ferrocene: the discovery and rediscovery of the sandwich complexes". *Angewandte Chemie*. 2012, vol. 51, no. 25, pp. 6052–6058.
2. Marks T.J., Fischer R.D. Synthesis, structure and properties of metal carbonyl tetrahydrofuran complexes of ferrocene. *J. Organomet Chem.*, 1998, vol. 212, no. 2, pp. 45–52.
3. Ibrahimova N.Z., Jafarov G.M., Taghiyev D.B., Lyatifov I.U. Research into kinetics of electron exchange reactions in the system sym. octamethylferrocene/sym. octamethylferricinium hexafluorophosphate.

- Chemical Problems*. 2019. vol. 17, no. 2. pp. 310–315.
- Malischewski M, Adelhardt M, Sutter J, Meyer K, Seppelt K. Isolation and structural and electronic characterization of salts of the decamethylferrocene dication. *Science*. 2016, vol. 353 (6300), pp. 678–682.
 - Anna Moysala, Albert G. Nasibulin, David P. Brown, Hua Jiang, Leonid Khriachtchev, Esko I. Kauppinen. Single-walled carbon nanotube synthesis using ferrocene and iron pentacarbonyl in a laminar flow reactor. *Chemical Engineering Science*, 2006, vol. 6 (13), pp. 4393–4402
 - Gubin S.P., Shulpin G.B. Methods for obtaining derivatives of iron clusters based on ferrocene. Novosibirsk, Nauka Publ., 1994, 286 p.
 - Thermodynamics of nanotubes /<https://elib.bsu.by/bitstream/123456789/223236/1/60-67.pdf>
 - Krol O.V., Druzhinina A.I., Varushchenko R.M., Zhizhko P.A., M. D. Reshetova M.D., Borisova N.E. and N. V. Chelovskaya N.V. *Russian Journal of Physical Chemistry A*. 2010, vol. 84, no. 5, pp. 771–777.
 - Krol O.V. Thermodynamic properties of some derivatives of ferrocene and perfluorooctaox-n-octadecane. Abstract diss. chemical sciences. Moscow-2007. https://new-dissert.ru/_avtoreferats/01003403107.pdf/
 - Olesya V. Krol, Anna I. Druzhinina, Raisa M. Varushchenko, Olga V. Dorofeeva, Marina D. Reshetova, Nataliya E. Borisov. The heat capacities and thermodynamic functions of some derivatives of ferrocene. *J. Chem. Thermodynamics*, 2008, vol. 40, pp. 549–557.
 - Michal Fulem, Kvetoslav Ruzicka, Ctirad Cervinka, Marisa A.A. Rocha, Luís M.N.B.F. Santos, Robert F. Berg. Recommended vapor pressure and thermophysical data for ferrocene. *J. Chem. Thermodynamics*. 2013, vol. 57, pp. 530–540.
 - Bulyarsky S.V., Pyatilova O.V., Tsygantsov A.V. Thermodynamics of the Formation of Clusters of Catalysts for the Growth of Carbon Nanotubes Electronics 2010, no.1(81), pp. 50–56.
 - Suleymanov G.Z., Gurbanov M.A., Akbarov A.Kh, Mammadova Z.M., Gochuyeva A.F. Synthesis of mono-, bi- and trinuclear carbinol derivatives of ferrocene, development of technologies obtaining of thin coverings of photocomposites with polymer matrixes and study of some electrophysical properties. *Azerbaijan Chemical Journal*, 2017, no. 4, pp. 48–54.
 - Mamedov A.N. Thermodynamics of systems with nonmolecular compounds. Calculation and approximation of thermodynamic functions and phase diagrams LAP Lambert Academic Publishing. 2015.115 c.
 - Shakhverdiev A.N., Mamedov A.N., Mekhdiev I.G., Safarov D.T., Khassel E.. Thermophysical properties and thermodynamic functions of molecular and non-molecular compounds and their solutions. Baku. Elm Publ., 2013, 313p.
 - Database. Thermal constants of substances. / <http://www.chem.msu.ru/cgi-bin/tkv.pl?show=welcome.html/welcome.html>
 - Zhang Q. Cai C., Qin J.W., and Wei B. Q. Tunable Self-discharge Process of Carbon Nanotube Based Supercapacitors. *Nano Energy*, 2014, vol. 4, pp. 14–22.
 - D.B. Tagiev, A.N. Mammadov. Promising Directions of Modern Chemistry. Baku, Elm Publ., 2014, 328 p.
 - Kim T. and Shima M. Reduced magnetization in magnetic oxide nanoparticles. *Journal of Applied Physics*, 2007, vol. 101, 09M516 <https://doi.org/10.1063/1.2712825>

ТЕРМИЧЕСКАЯ УСТОЙЧИВОСТЬ И ТЕРМОДИНАМИКА ПИРОЛИЗА МОНО-, БИ- И ТРЕХЯДЕРНЫХ КАРБИНОЛЬНЫХ ПРОИЗВОДНЫХ ФЕРРОЦЕНА

А.И. Рустамова¹, З.Г. Курбанов², З.М. Мамедова¹, С.Н. Османова¹, А.Х. Кулизаде¹,
А.Н. Мамедов^{1,3}, Э.Г. Исмаилов¹

¹*Институт Катализа и Неорганической химии им.М. Нагиева.*

пр. Г.Джавида, 113, AZ1143, Баку, Азербайджан;

²*SOCAR Downstream Management, Баку, Азербайджан;*

³*Азербайджанский Технический Университет,*

просп. Г.Джавида. 25, AZ-1073 Баку, Азербайджан

aygun.rustamova1601@gmail.com

Аннотация: Синтезированы моно-, би- и трехядерные карбинольные производные ферроцена $C_5H_5FeC_5H_4-C(CH_3)_2OH$ (I), $[C_5H_5FeC_5H_4]_2C(CH_3)OH$ (II), $[C_5H_5FeC_5H_4]_3C-OH$ (III). изучены термическая стабильность и термодинамика пиролиза этих соединений. Состав и строение синтезированных соединений установлены методами элементного анализа (ААС, С, Н-анализ), ЯМР ¹H, ИК- и УФ/видимой спектроскопии. В ИК-спектрах этих соединений присутствуют полосы поглощения с $\nu(OH) = 2910-3040\text{ см}^{-1}$ и $\nu(OH) = 3080-3190\text{ см}^{-1}$, а в спектрах ¹H ЯМР – полосы поглощения со значениями химического сдвига $\delta(OH) = 4,29-4,18$ м.д. для ОН-групп, различающихся по положению и обусловленных образованием внутри- и межмолекулярных ассоциатов с участием ОН-групп. Электронные спектры поглощения свидетельствуют о наличии в соединениях I–III характерных полос поглощения при $\lambda_{max} = 270$ (I), 278 (II) и 285 нм (III). Показано, что при прогреве образцов от комнатной температуры до 700°C в токе инертного газа остаточная масса для соединений I–III составляет, соответственно, 2,05, 20,24 и 66,96% от исходной массы и эти соединения разлагаются с образованием наноразмерных частиц железа/оксида железа и углерода. Вычислены значения температуры плавления и намагниченности насыщения наноразмерных частиц железа, образующихся при пиролизе ферроцена и его производных I–III.

Ключевые слова: карбинол производные ферроцена, термическая устойчивость, пиролиз

FERROSENİN MONO-, Bİ- VƏ ÜÇNÜVƏLİ KARBİNOL TÖRƏMƏLƏRİNİN TERMİKİ STABİLLİYİ VƏ PİROLİZİNİN TERMODİNAMİKASI

A.I. Rüstəmovə¹, Z.H. Qurbanov², Z.M. Məmmədova¹, S.N. Osmanova¹, A.X. Quluzadə¹,
A.N. Məmmədov^{1,3}, E.H. İsmayilov¹

¹*Akad. M.Nağıyev adına Kataliz və Qeyri-üzvi Kimya İnstitutu,*

H.Cavid pr., 113, AZ1143, Bakı, Azərbaycan;

²*SOCAR Downstream Management, Bakı, Azərbaycan;*

³*Azərbaycan Texniki Universiteti,*

H. Cavid prosp. 25, AZ-1073 Bakı, Azərbaycan

aygun.rustamova1601@gmail.com

Xülasə: Ferrosenin mono-, bi- və üçnüvəli karbinol törəmələri $C_5H_5FeC_5H_4-C(CH_3)_2OH$ (I), $[C_5H_5FeC_5H_4]_2C(CH_3)OH$ (II), $[C_5H_5FeC_5H_4]_3C-OH$ (III) sintez edilmiş, onların termiki davamlılığı və pirolizinin termodinamikası tədqiq edilmişdir. Sintez edilmiş birləşmələrin tərkibi və quruluşu element analizi (AAS, C,H analizi), ¹H NMR, İQ və UB/görünən sahə spektroskopiyası metodları ilə müəyyən edilmişdir. Bu birləşmələrin IQ spektrlərində müşahidə olunan $\nu(OH) = 2910-3040\text{ sm}^{-1}$ və $\nu(OH) = 3080-3190\text{ sm}^{-1}$ udma zolaqlarına aid və ¹H NMR spektrlərində kimyəvi sürüşmə qiymətləri $\delta(OH) = 4.29-4.18$ ppm intervalında dəyişən OH qruplarının iştirakı ilə molekul daxili və intermolekulyar assosiasiyaların

mövcudluğu ehtimal edilir. I-III birləşmələri üçün xarakterik elektron udma spektrlərinin $\lambda_{\max} = 270$ (I), 278 (II) və 285 nm (III) olduğu göstərilmişdir. Göstərilmişdir ki, nümunələr inert qaz axınında otaq temperaturundan 700 °C-ə qədər qızdırıldıqda, I-III birləşmələri üçün qalıq kütlə ilkin kütlənin müvafiq olaraq 2.05, 20.24 və 66.96%-ni təşkil edir və bu birləşmələr dəmir/dəmir oksidi və karbonun nanoölçülü hissəciklərinin əmələ gəlməsi ilə parçalanır. Ferrosen və onun I-III törəmələrinin pirolizi zamanı əmələ gələn nanoölçülü dəmir hissəciklərinin ərimə temperaturu və maqnitlənmə doyumunun qiymətləri hesablanmışdır.

Açar sözlər: ferrosen, karbinol törəmələri, termiki sabillik, piroliz.